GENERATION OF ELASTIC WAVES BY

ELECTROMAGNETIC INDUCTION

D. J. Mayton*† and William P. Winfree
MS 231
NASA Langley Research Center
Hampton, VA 23665

INTRODUCTION

Photoacoustics in solids provides a useful technique for both characterization of material properties and the detection of defects. In photoacoustics, a periodic thermal source is used to generate an elastic wave. Typically the thermal source is a laser or charged particle beam, however other sources are currently being investigated. A need for other sources is required for objects which have reflective surfaces or are too large to fit into a vacuum chamber, such as large metallic structures.

For metallic structures, inductive heating may provide an appropriate thermal source. Inductive heating occurs when a time varying magnetic field is coupled into a conductor. Since the interaction is between the conductor and the magnetic field to approximately the skin depth of the material, no coating is required to absorb the energy. In addition the power is easily modulated and a coil can be tailored to reach areas of the structure inaccessible to other sources.

This paper investigates the generation of elastic waves in a conductor with induction heating. Elastic waves were generated in an aluminum rod and detected with an accelerometer. The technique is shown to be able to detect simulated defects far below the thermal wavelength or the skin depth for the respective excitation frequencies. Section II discusses the technique for generating and detecting the elastic waves. A series of measurements on rods with different depth defects is reported in section III.

MEASUREMENT SYSTEM

Inductive heating results from the resistance of a conductor to eddy currents induced by a time varying magnetic field. To efficiently couple a magnetic field into a conductor, a portion of a toroid core was removed and the remainder wrapped with wire as shown in figure 1. The core was driven with a broad band power amplifier with a 50 ohm output impedance. To increase the efficiency of the system, capacitors were added in parallel and series to the core on the sample, forming a tank

---

*Analytical Services and Materials, Inc.
† current address Department of Materials Science and Engineering, 102 Maryland Hall, Johns Hopkins University, Baltimore MD 21218

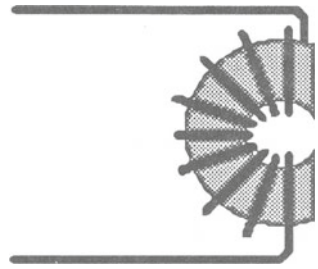

Figure 1. Cross section of typical toroid core used for coupling the magnetic field into the sample.

circuit with an impedance of 50+-13 ohms at a resonant frequency between 100Khz and 1 Mhz. The tank circuit was then driven at its resonant frequency to give an inductive heating source.

Photoacoustics has demonstrated elastic waves can be generated by periodically cycling a thermal source. For the inductive source described above this was easily obtained by amplitude modulating the drive at a frequency at least 2 decades below the drive frequency. The generated elastic wave was then detected by an accelerometer attached to the sample. The accelerometer signal after charge amplification was input into a lockin detector which was synchronously detecting at the modulation frequency of the drive. To obtain a signal which was above the noise, the modulation frequency was varied until a resonance of the sample, described later, was located.

To simulate the process used in photoacoustics, the core was mounted on a computer controlled scanner arm, so that the thermal source could be scanned over the sample surface. A length of the sample was then scanned with the coil and the in phase and quadrature signals from the accelerometer recorded as a function of position along the rod. The measurement system with a rod mounted is shown in figure 2.

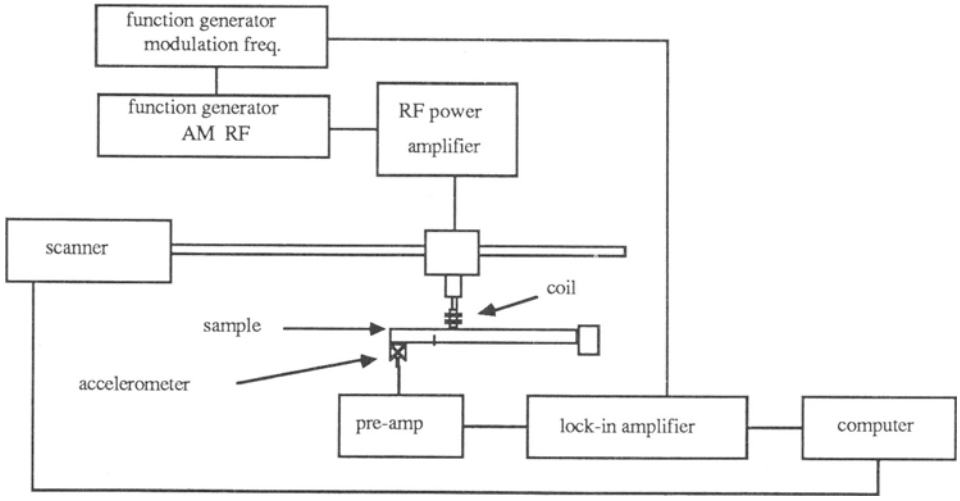

Figure 2. Experimental setup for scanning induction heating source across sample with defect.

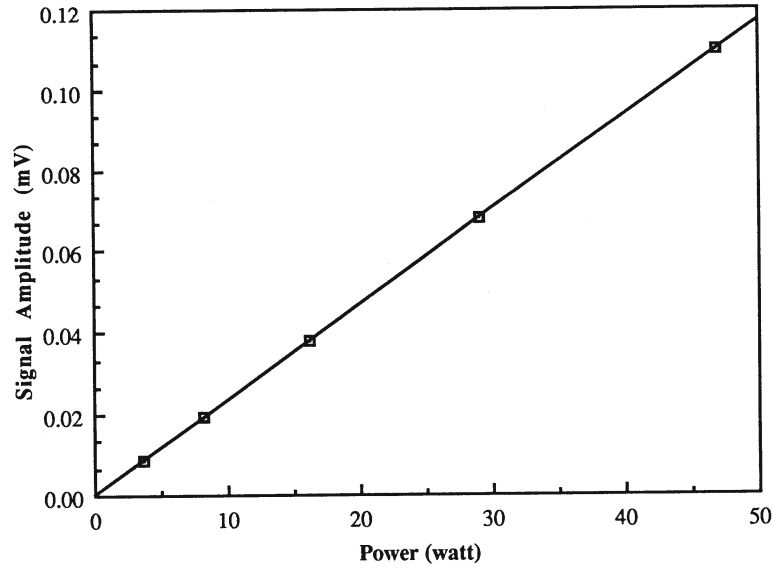

Figure 3. Amplitude of signal received at accelerometer as a function of power to the toroid core.

RESULTS AND DISCUSSION

In photoacoustics, an elastic wave generated by a thermal source has an amplitude which is proportional to the thermal expansion of the solid. Since the thermal expansion is linearly proportional to the power absorbed by the solid, a signal resulting from a thermally generated elastic wave is proportional to the input power rather than the input amplitude. To demonstrate that the elastic wave generated by the induction heating is the result of a thermally induced strain as is the case for photoacoustics, the power applied to the coil was varied and the amplitude of the received signal was measured. The data, shown in figure 3 with a straight line drawn for comparison, indicates the signal is thermally induced, and therefore can be analysed in a manner similar to photoacoustics.

Measurements were then made by scanning the coil over a 1.27 cm square aluminum rod which was 101.6 cm long and mounted at both ends. The accelerometer was secured to the center of the rod by drilling a hole through the rod and screwing the accelerometer to the back. The head of the screw was recessed to allow scanning over the length of the rod. A 0.1 cm wide, 0.9 cm deep band saw cut 17.5 cm from the center of the rod formed a slot which simulated a defect.

A thermally induced strain will exist principally to a depth of one thermal diffusion length into the sample. The thermal diffusion length for the lowest modulation frequency (144 Hz) was found to be much less than the width of the rod (~0.07 cm). Therefore the thermally induced strain is confined to one side of the rod, generating a bending which can excite transverse waves and modes.

If a transverse wave is excited in a slender rod with both ends rigidly bound, the frequencies of the normal modes are given by the roots of the equation

$$1 - \cosh(k l) \cos(k l) = 0 \qquad (1),$$

Table I. Calculated and measured frequencies for first seven modes of 101.6 cm long, 1.27 cm square aluminum rod.

Mode #	Calculated frequency (Hz)	Observed frequency (Hz)
1	64	
2	178	144
3	350	305
4	579	510
5	865	752
6	1208	1187
7	1609	1464

where l is the length of the rod, and k is given by the expression

$$k = \frac{12\,\rho}{Y\,W^2}\,\omega^{1/2} \qquad (2),$$

where Y is the Young's modulus, W is the width of the rod, ρ is the density and ω is the angular frequency. For the long aluminum rod bound at both ends, the frequencies of the first few modes are given in table 1, with corresponding modulation frequencies of resonances found close to these values. For all cases the measured value was found to be lower than expected for a perfect rod. The rod, of course, was far from perfect, with a hole drilled through the center, a mounted accelerometer, and a slot which was 70% of the thickness of the rod deep.

The amplitude of displacement for the normal modes of a slender rod is given by the expression

$$\eta(x) = A[\sinh(k\,x) + \sin(k\,x)] + B[\cosh(k\,x) - \cos(k\,x)] \qquad (3),$$

where

$$A = B\,\frac{\cosh(k\,l) - \cos(k\,l)}{\sinh(k\,l) - \sin(k\,l)} \qquad (4).$$

The displacement of mode 5 as a function of position is shown in figure 4, along with the in phase and quadrature signals measured for the modulation frequencies found to excite a resonance closest to these modes. The calculated displacements correlate with the quadrature signal for all modes and this suggests that for a perfect rod, all the measured signal would be quadrature to the modulation. The correlation between calculated displacements and measured signals, and the correlation between measured and calculated mode frequencies, indicate that the thermally induced strain is exciting transverse waves in the rod.

For transverse waves propagating along a slender rod, a change in the dimension of the rod changes the phase velocity and impedance of the rod. A wave propagating across an interface between a thick segment of the rod to a thinner segment would therefore be partially reflected and partially transmitted. If this thinning exists only for a short segment of the rod compared to the wavelength of the transverse wave, the effect

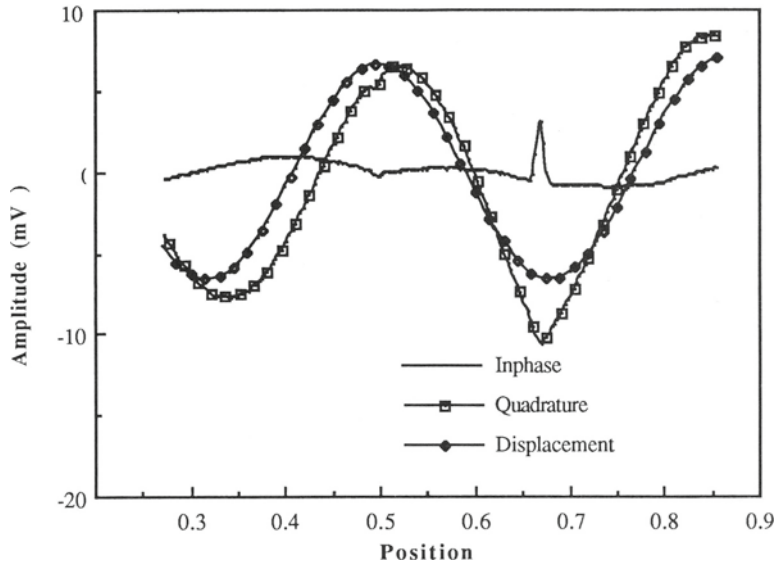

Figure 4. The inphase and quadrature signals for 752 hz mode as a function of position of the toroid normalized to the length of the rod.

is small, and increases as the wavelength decreases. The slot produces a thin segment in the rod. The effect of this thinning of the rod can be seen in both the in phase and quadrature signals, however is more pronounced in the quadrature signal. It is apparent that the transverse waves are being reflected off the defect and that these reflections can be detected a considerable distance from the defect. A second result of thinning a segment of the rod occurs when the elastic wave is generated over the thinner section, and since the width of the rod has decreased, the magnitude of the bending is greater. This results in a localized effect as the core traverses over the defect, and can easily be seen in the data.

The shape of this signal contains information on core size, defect size, and the rod dimension. To identify the contribution from the core size, four different footprint sizes were used to excite the elastic waves and measurements were taken over the segment with the slot. As the size of the footprint increased, the signal level amplitude decreased for the same input power. To compare the different footprint sizes, the phase shift between received signal and source was measured as a function of position with a modulation frequency of 752 Hz. The width of the signal peak increases and the magnitude decreases as the footprint size increases. The width of each peak as a function of footprint size is a quantitative indicator of the core size's effect on the resolution of the system and is shown in table II. The minimum width obtainable for

Table II. Width of localized signal due to defect as a function of size of toroid core footprint.

Footprint Size(cm)	Width of signal(cm)
0.25	0.85
0.50	1.02
1.10	1.87
1.80	3.05

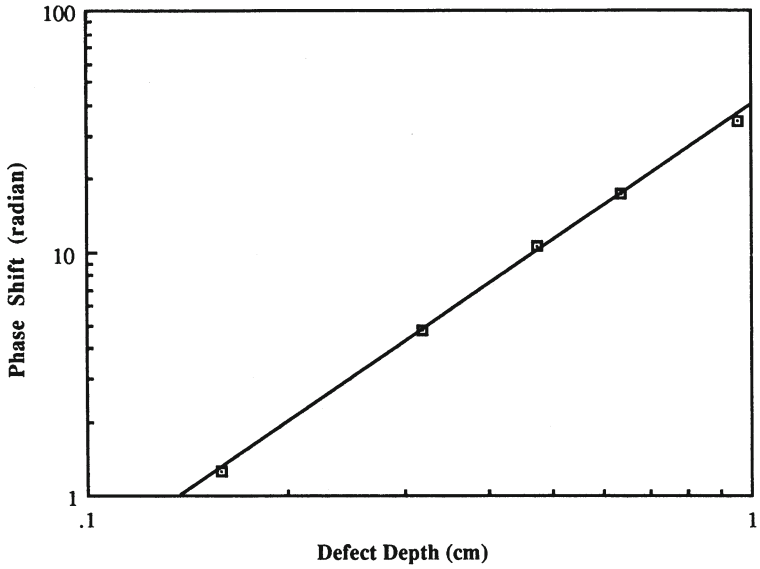

Figure 5. Amplitude of phase shift in the received signal as the core passed over the defect for slots of difference depths from the back side of the rod. Plotted with the data is a log fit to the data indicating the phase shift goes as the depth of the slot to approximately 1.9 power.

this system was approximately one half the width of the rod. As can be seen from the table, after reducing the size of the core to about one quarter the size of the rod, further reductions will not significantly increase the resolution of the system.

In order to determine the contribution of defect depth to the signal shape, a series of 9 shorter rods with simulated defects varying in depth and position were tested. These aluminum rods were all 30.5 cm long with 0.1 cm wide band saw cuts. These samples were divided into two sets to examine two different affects of the simulated defect on the observed signal. For one set, each rod had a slot cut at a different location, all the approximately 75% of the thickness of the rod. For the second set, each rod had a slot cut to a different depth at 6.72 cm from the free end of the rod. The samples were mounted in the system with only one end clamped and a accelerometer attached, using phenol salicilate, to the free end. Phase shift relative to the source was then measured as a function of position and the natural log of these results for bars 1-6 are shown in figure 5. The slope of the best fit line is about 1.9 indicating a power relationship of 1.9 between the phase shift and defect depth.

Since the presence of the slot results in a reduction in the effective stiffness of the rod as a whole, it would be expected to reduce the resonant frequency of the rod. This expected trend can be seen in the measurements of the resonant frequency as a function of slot size shown in figure 6. This is true, however, only if the slot occurs in a region of large strain. As the slot moves towards the center of the rod, which is a nodal point in the transverse standing wave, its effect on the resonant frequency decreases, and the resonant frequency approaches that of a rod with no slot. This can be clearly seen from the measurement of

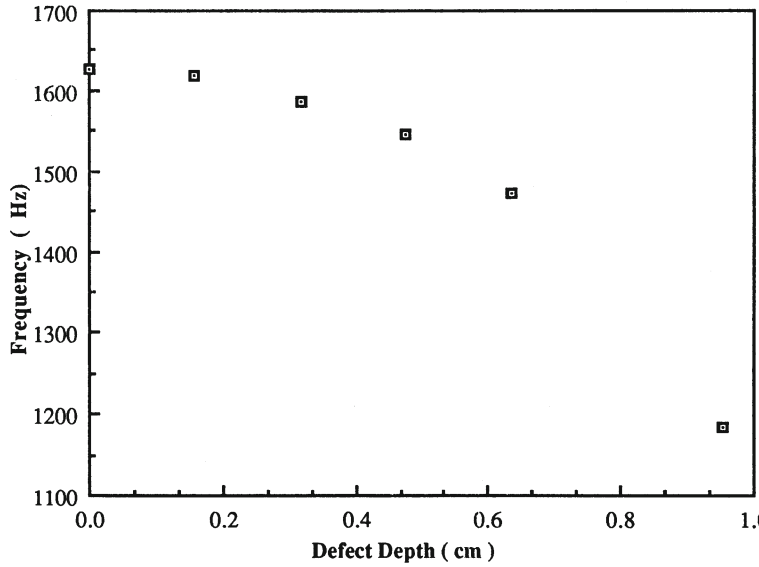

Figure 6. Resonant frequency of rod measured for the series of rods with the slots to different depths.

resonant frequency as a function of position in figure 7. Sufficient modal analysis at several different frequencies could detect the size and position of such a defect, with the excitation at a single point and the measurement at a single point, as has been demonstrated elsewhere.

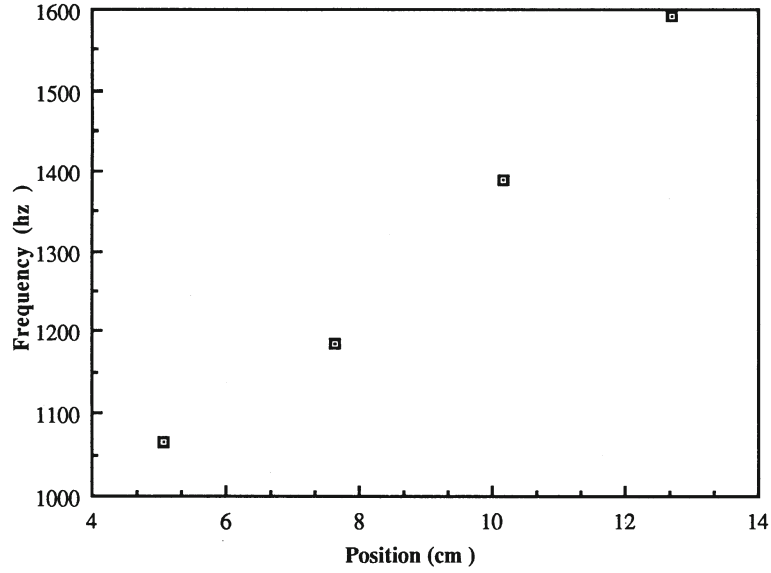

Figure 7. Resonant frequency of rod measured for the series of rods with the slots to different distances from the end of the rod.

SUMMARY

It has been shown that it is possible to generate elastic waves by induction heating in a conductor. For the case of a rod, it is possible to excite transverse waves at different positions along the sample and detect them far from the source. The transverse waves reflect off defects perturbing the normal modes of the rod. Both the depth and position of the defect effect the resonant frequency of the rod. In addition, a defect in the rod changes the magnitude of the bending as well as the phase shift between input signal and response as a thermal source passes over it.